ARTICLES

Metal-Enhanced Fluorescence of Phycobiliproteins from Heterogeneous Plasmonic Nanostructures

Mustafa H. Chowdhury,[†] Krishanu Ray,[†] Kadir Aslan,[‡] Joseph R. Lakowicz,[†] and Chris D. Geddes*,[‡]

Center for Fluorescence Spectroscopy, Medical Biotechnology Center, University of Maryland School of Medicine, 725 West Lombard Street, Baltimore, Maryland 21201, and Institute of Fluorescence, Laboratory for Advanced Medical Plasmonics, & Laboratory for Advanced Fluorescence Spectroscopy, Medical Biotechnology Center, University of Maryland Biotechnology Institute, 725 West Lombard Street, Baltimore, Maryland 21201

We report here the use of plasmonic metal nanostructures in the form of silver island films (SiFs) to enhance the fluorescence emission of five different phycobiliproteins. Our findings clearly show that the phycobiliproteins display up to a 9-fold increase in fluorescence emission intensity, with a maximum 7-fold decrease in lifetime when they are assembled as a monolayer above SiFs, as compared to a monolayer assembled on the surface of amine-terminated glass slides of the control sample. The study was also repeated with a thin liquid layer of the phycobiliproteins sandwiched between two glass substrates (and a SiFs and a glass substrate) clamped together. Similarly, the results show a maximum 10-fold increase in fluorescence emission intensity coupled with a 2-fold decrease in lifetime of the phycobiliproteins in the SiF−glass setup as compared to the glass control sample, implying that near-field enhancement of phycobiliprotein emission can be attained both with and without chemical linkage of the proteins to the SiFs. Hence, our results clearly show that metal-enhanced fluorescence (MEF) can potentially be employed to increase the sensitivity and detection limit of the plethora of bioassays that employ phycobiliproteins as fluorescence labels, such as in fluoro-immunoassays where the assay can be tethered on the surface of SiFs, and also in flow cytometry where analytes in the liquid phase could potentially flow through channels coated with SiFs without actually being attached to the silver.

1. Introduction

Phycobiliproteins are unique photosynthetic pigment−protein complexes found in cyanobacteria and red algae.[1−13] They play a crucial role in efficiently harvesting sunlight that chlorophylls poorly absorb and then transfer this energy via a series of energy transfer mechanisms to chrolophyll in the membranes of these organisms.[1−13] In cyanobacteria and red algae, the phycobiliproteins are found in supramolecular aggregates called phycobilisomes that are attached to the outer surface of the photosynthetic membrane.[1−13] These proteins absorb visible light from 450 to 650 nm and are classified into three types based on their absorption spectra: phycoerythrin (PE), phycocyanin (PC), and allophycocyanin (APC).[1−13] Phycobiliproteins possess several unique characteristics that make them attractive for use as fluorescence labels in the analysis of biomolecules and cells.[2,3,5] (i) They contain multiple bilin chromophores and hence have high absorbance coefficients over a wide region of the visible spectra (ϵ_M for B-PE = 2.4×10^6 cm^{-1} M^{-1} at 543 nm); (ii) they have high fluorescence quantum yields, which are remarkably constant over broad pH range (quantum yield

~ 0.98 for B-PE); (iii) they have strong absorption bands that start at ~440 nm and have strong emission bands that begin at 550 nm and extend well into the red region of the visible spectrum, where interference from biological molecules is minimal; (iv) large Stokes shift that minimizes interferences from Rayleigh and Raman scatter and other fluorescing species; (v) most biomolecules do not quench their fluorescence; (vi) they have high solubility in aqueous solutions; and (vii) they are also stable in solution and in the solid phase and thus can be stored for long periods on the shelf.[2,3,5,11]

For the reasons described, phycobiliproteins have subsequently been used widely in a variety of fluoro-immunoassays.[11,14] The natural ability of phycobiliproteins to participate in efficient fluorescence-resonance energy processes (FRET) have also been exploited in various FRET assays with commercially available antibodies, and also in flow cytometry applications to study arrays of biomolecules and multimolecular complexes.[10,11,15] Phycobiliprotein-Fab conjugates have also been used in single particle fluorescence imaging (SPFI) applications for observing cell receptor movement and associations at high spatial resolution on the surface of living cells.[16,17] Phycobiliproteins have also been the focus of several single molecule spectroscopy studies and also have been used in high-speed high-throughput single-molecule imaging techniques for

---

 * Corresponding author. Fax: (410) 706-4600. E-mail: geddes@umbi.umd.edu.
 † University of Maryland School of Medicine.
 ‡ University of Maryland Biotechnology Institute.

Metal-Enhanced Fluorescence of Phycobiliproteins

J. Phys. Chem. C, Vol. 111, No. 51, 2007 **18857**

identifying in free solution biomolecules, a technique with potential for use in high-speed detection of specific disease markers.[12,18,19] Hence, further enhancing the fluorescence emission properties and improving the photostability of phycobiliproteins will serve to make them even more efficient labels in the analysis of biomolecules and cells. This can be possible via utilizing the close-range (within 100 nm) interactions of these proteins with plasmonic nanoparticles.

The first description of the interactions of metal−fluorophore was reported by Drexhage in 1974,[20] whereby the enhanced fluorescence intensities and decreased lifetimes were later thought to occur due to the changes fluorophore's radiative decay rate. Subsequently, many applications of radiative decay engineering (RDE) to biological problems have been realized.[21−25] In 2002, RDE was renamed metal enhanced fluorescence (MEF)[26] that also takes into account other effects such as enhanced absorption.[27−35] More recently, a new explanation of plasmonic nanoparticle−fluorophore interactions was described by the radiating plasmon (RP) model,[36−37] where the observations of enhanced emission and decreased lifetimes are due to the coupling of the fluorophores at their excited state with surface plasmons of the nanoparticles.[36,37] According to this model, the emission or quenching of a fluorophore near the metal can be predicted by the optical properties of the metal structure as calculated from electrodynamics and Mie theory.[36−38]

Our current understanding of MEF underpins the RP model, according to which optically excited fluorophores induce surface plasmons (mirror dipoles) in silver nanoparticles, which in turn radiate the spectral properties of the excited state.[36,37] Subsequently, we have developed the RP model and have also demonstrated its plausibility experimentally.[37] In these experiments, larger silver nanostructures have been shown to be more efficient at coupling and therefore radiating fluorescence than smaller ones.[29] It is well known that the extinction properties (C_E) of metal nanoparticles can be expressed as both a combination of both absorption (C_A) and scattering (C_S) factors.[36−39] In the simplest case, when the particles are spherical and have sizes comparable to the incident wavelength of light, that is, in the Mie limit, the extinction can be expressed as[36,37]

$$C_E = C_A + C_S = k_I \, \text{Im}(\alpha) + \frac{k_1}{6\pi} |\alpha|^2 \qquad (1)$$

where $k_1 = 2\pi \, n/\lambda_0$ is the wavevector of the incident light in the medium and α is the polarizability of a sphere with radius r, n is the refractive index of the medium, and λ_0 is the incident wavelength in the medium. The term α is the polarizability of a sphere of radius r and can be expressed as[36]

$$\alpha = 4\pi \, r^3 (\epsilon_m - \epsilon_1)/(\epsilon_m + 2\epsilon_1) \qquad (2)$$

where ϵ_m and ϵ_1 are the complex dielectric constants of the metal and the media, respectively. We believe MEF is based on the scattering components of the metal extinction (C_S in eq 1), that is, the ability of fluorophore-induced plasmons to radiate (plasmon scatter). An examination of eqs 1 and 2 shows that C_A increases as r^3, whereas C_S increases as r^6. For this reason, we expect larger metal nanoparticles to have a larger scattering component, and so preferable for metal-enhanced fluorescence, whereas small metal nanoparticles are expected to quench fluorescence because the absorption component dominates over scattering. Hence, a plasmon induced by fluorophores in a metallic nanostructure with a large scattering component (C_S) will radiate the photophysical properties of the excited state intensely, thereby leading to observations of emission enhance-

ments (high apparent system quantum yields, where system = excited-state fluorophore/metal nanoparticle complex) even from fluorophores with high free space quantum yields such as phycobiliproteins. The ability of a metal surface to scatter or absorb light (i.e., enhance or quench fluorescence) can also be attributed to wavevector matching requirements at the metal−fluorophore interface.[36] This wavevector matching requirement can be manipulated by adjusting the sample conditions to obtain enhanced fluorescence emission. Hence, the RP model provides a rational approach for designing fluorophore−metal configurations with the desired emissive properties.[22]

In this current study, we use metallic nanostructures, that is, silver island films (SiFs) to enhance the fluorescence emission of the following phycobiliproteins: R-phycoerythrin (R-PE), B-phycoerythrin (B-PE), allophycocyanin (APC), cross-linked allophycocyanin (XAPC), and C-phycocyanin (C-PC). Our findings show that the phycobiliproteins display an appreciable increase in fluorescence emission intensity and decrease in lifetime when they were assembled as a monolayer on the surface of SiFs as compared to a monolayer assembled on the surface of amine-terminated glass slides, that is, a control sample by which to compare the enhancement effect. The study was also repeated with a thin liquid layer of the phycobiliproteins sandwiched between two glass substrate (and a SiFs and glass substrate) held together with a clamp. In this experimental configuration, the results also indicate an appreciable increase in fluorescence emission intensity and decrease in lifetime of the phycobiliproteins in the SiF−glass setup as opposed to the glass−glass configuration. The results indicate that enhancement of phycobiliprotein emission can be attained with and without chemical linkage of the proteins to the SiFs. Hence, this study strongly suggests that metal-enhanced fluorescence (MEF) can be employed to increase the sensitivity, photostability, and detection limit of the plethora of bioassays that employ phycobiliproteins as fluorescence labels.

2. Experimental Section

2.1. Materials. R-phycoerythrin (R-PE), B-phycoerythrin (B-PE), allophycocyanin (APC), cross-linked allophycocyanin (XAPC), and C-phycocyanin (C-PC) supplied in a 100 mM sodium phosphate buffer with 60% ammonium sulfate and 0.02% sodium azide were purchased from Cyanotech Corporation (Kailua-Kona, HI). Standard microscope glass slides (75 × 25 mm) used for silver island film (SiF) preparation were purchased from VWR Scientific (West Chester, PA). Nanopure water (>18.0 MΩ) purified using a Millipore Milli-Q gradient system was used in all of the experiments. All other compounds, including premium-quality APS-coated (amine-terminated) glass slides (75 × 25 mm), sodium phosphate, 2-aminothiophenol, silver nitrate, ammonium hydroxide, sodium hydroxide, and glucose were purchased from Sigma-Aldrich (St. Louis, MO) and used as received.

2.2. Purification of Phycobiliproteins. The phycibiliproteins as received from the manufacturer were spun down in Centricon Plus-20 Centrifugal Filters Devices (100 000 MWCO) (Millipore, Billerica, MA) at 10 000 RPM for 10 min in a Beckman Avantio J-25 I centifuge (GMI Inc., Ramsey, MN). The precipitate was then redissolved in 100 mM sodium phosphate buffer, pH 7.0. The final concentration of the purified phycobiliprotein solution used in the experiments was calculated using their absorption spectra, which were measured using a Hewlett-Packard 8453 spectrophotometer. The concentrations of the phycibiliprotein solutions after purification were approximately as follows: R-phycoerythrin (R-PE), 4 μM; B-phycoerythrin

(B-PE), 3 μM; allophycocyanin (APC), 8 μM; cross-linked allophycocyanin (XAPC), 4 μM; and C-phycocyanin (C-PC), 4 μM.

2.3. Silver Island Film (SiF) Preparation. The glass slides (Corning, NY) used for silver island film (SiF) preparation were first cleaned by soaking them overnight in a 10:1 (v/v) mixture of H_2SO_4 (95−98%) and H_2O_2 (30%) (commonly known as piranha solution). After being washed rigorously with MilliQ deionized water, the glass slides were air-dried. SiFs were deposited on the clean glass slides via a method based on previous reports.[40] Briefly, about 1.5 mL of freshly prepared 5% NaOH solution was added to a stirring aqueous silver nitrate solution (0.375 g in 45 mL of water) in a glass beaker. Subsequently, the resulting dark-brown precipitate was redissolved by slowly adding 1 mL of NH_4OH. The solution was cooled to 5 °C in an ice bath and a fresh solution of D-glucose (0.540 g in 11 mL of water) was added, followed by four pairs of dried glass slides placed into this solution. The mixture was stirred for 2 min in an ice bath and then allowed to warm to 30 °C for the next 5 min. As the color of the mixture turned from yellow-greenish to yellow-brown, the color of the slides became greenish. The slides were removed from the beaker and rinsed with Milli-Q water. Excess and nonadhesive silver particles on the glass surface were removed by mild sonication of the SiF-coated glass slides for 1 min. The SiF slides were stored in Milli-Q water until they were used. We used the SiFs in our experiments within 2 days of forming them. After 2 days of storage in Milli-Q water, we did not see a change in the surface plasmon resonance of the SiFs, both showing an extinction maximum at roughly 460 nm (measured right after formation and after 2 days of storage in water, data not shown), an hence can negate any detrimental effects of major oxide layer formations on our SiFs. The diameters of the islands are typically 100−500 nm across and some 60 nm high.[22,40]

2.4. Formation of a Monolayer of Phycobiliproteins on Amine-Terminated Glass Slides and SiFs. The commercially purchased amine-terminated glass slides were used after drying with air to remove dust particles from the surface. The SiFs were incubated overnight with 1 mM solution of 2-aminothiophenol in methanol and then rinsed with copious amount of methanol and Milli-Q water. This step forms a self-assembled monolayer of aminothiophenol on the surface of the SiFs. The functionalized glass and SiFs were then incubated with approximately 200 μL of the respective phycobiliproteins overnight and then rinsed with 100 mM sodium phosphate buffer (pH 7.0) to remove any unbound protein. It is thought that the phycobiliproteins form a monolayer on the surface of the functionalized glass and SiFs through nonspecific binding, similar to reports on other proteins by the authors.[22−27] The protein monolayer on the glass and SiFs was coated with approximately 50 μL of sodium phosphate buffer, covered with a coverslip, and clamped before performing fluorescence experiments. It was deemed important to keep the phycobiliprotein surface wet with buffer at all times in order to prevent protein denaturation, which could potentially lead to irreversible conformation changes in the protein, which in turn might affect its fluorescence properties.

2.5. Formation of a Thin Liquid Layer of the Phycobiliproteins Sandwiched between Two Glass Substrates and a SiF and Glass Substrate. Approximately 100 μL of the different phycobiliprotein solutions were sandwiched between two amine-terminated glass slides and a SiF and a glass slide, respectively. This formed a thin liquid layer of the phycobiliproteins sandwiched between two glass slides, and the SiF and

glass, respectively. Typically, the space between two sandwiched slides was ∼1 μm, confirmed by absorption path length studies.[22]

2.6. Fluorescence Studies. Fluorescence spectra of the monolayer and liquid sandwich samples were collected after mounting the samples on a stand, the spectra recorded with a model SD 2000 Ocean Optics spectrometer (Dunedin, FL) connected to an Ocean Optics low OH 1000 μm diameter optical fiber with NA of 0.22. A 473 nm diode laser was used for exciting the R-PE and B-PE samples, and a Coherent 638 nm diode laser (Santa Clara, CA) was used for the APC, XPC, and C-PC protein samples. The photostability studies were performed on the monolayer samples for 600 s.

Time-resolved intensity decays were recorded with a Pico-Quant Fluotime 100 time-correlated single-photon counting (TCSPC) fluorescence lifetime spectrometer (Berlin, Germany). The excitation at ∼473 nm (for R-PE and B-PE) was obtained using a pulsed laser diode (PicoQuant PDL800-B) with a 20 MHz repetition rate; the excitation at ∼633 nm (for APC, XAPC, and C-PC) was obtained using a pulsed laser diode (PicoQuant PDL800-B) also with a 20 MHz repetition rate. The instrument response function (IRF) was about 300 ps. The excitation was vertically polarized, and the emission was recorded through a polarizer oriented at 54.7°, the magic angle. Appropriate band-pass filters at 530−585 nm and 640−680 nm from Chroma Technology Group (Rockingham, VT) were used for collection, thus eliminating the scattered excitation light and collecting the fluorescence from the samples in the region of interest.

2.7. Data Analysis. The fluorescence intensity decays were analyzed in terms of the multiexponential model as the sum of individual single-exponential decays:[13]

$$I(t) = \sum_{i=1}^{n} \alpha_i \exp(-t/\tau_i) \tag{3}$$

In the above expression, τ_i are the decay times and α_i are the amplitudes and $\Sigma_i \alpha_i = 1.0$. The fractional contribution of each component to the steady-state intensity is described by

$$f_i = \frac{\alpha_i \tau_i}{\sum_j \alpha_j \tau_j} \tag{4}$$

The mean (intensity weighted) lifetime is represented by

$$\bar{\tau} = \sum_i f_i \tau_i \tag{5}$$

and the amplitude weighted lifetime is given by

$$\langle \tau \rangle = \sum_i \alpha_i \tau_i \tag{6}$$

The values of α_i and τ_i were determined using the PicoQuant Fluofit 4.1 (Professional Version) software with the deconvolution of instrument response function and nonlinear least-squares fitting. The goodness-of-fit criterion was determined by the χ^2 value.[13]

3. Results and Discussion

Figure 1 shows the fluorescence emission spectra from a monolayer of R-phycoerythrin (R-PE) on glass and SiFs. The results show an approximately 7-fold increase in fluorescence
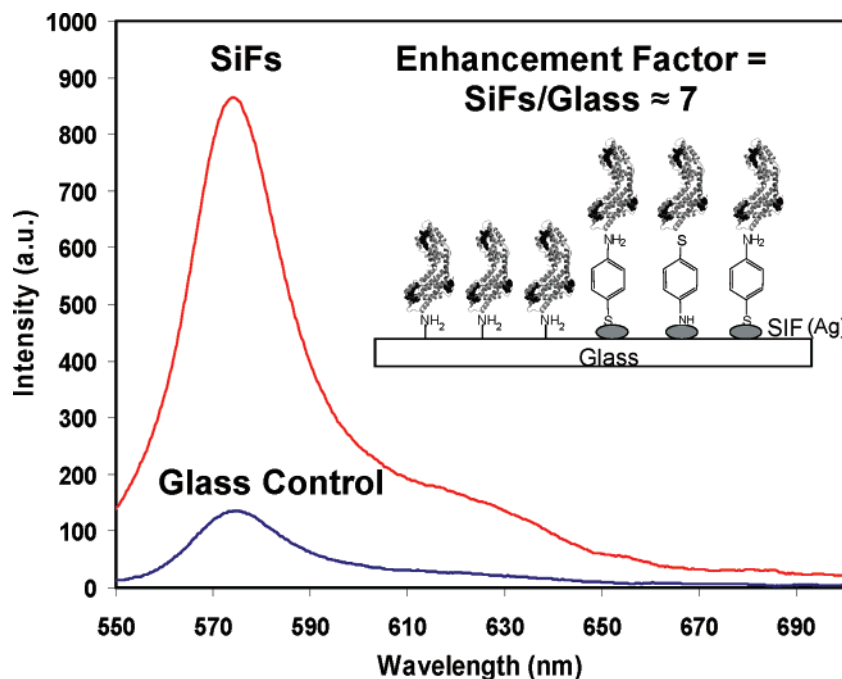
Metal-Enhanced Fluorescence of Phycobiliproteins

J. Phys. Chem. C, Vol. 111, No. 51, 2007 **18859**

Figure 1. Fluorescence emission spectra from a monolayer of R-phycoerythrin on glass and SiFs. (Inset) Experimental configuration. SiFs = silver island films.

intensity on SiFs, as compared to a control sample containing no surface silver nanostructures. The inset in the figure is a diagram showing the experimental configuration with the monolayer of the proteins anchored to the functionalized glass and SiFs. This finding suggests that this approach may be of significance for optically amplifying phycobiliprotein fluorescence-based bioassays, potentially increasing sensitivity and thus analyte/biospecies detectability. Given that the free-space quantum efficiency of R-PE is 84% (0.84 quantum yield), we acknowledge that at first glace it might seem improbable to have a 7-fold enhancement in emission intensity on SiFs because this would suggest a fluorophore quantum efficiency of 588% on SiFs.[13] This interesting phenomenon can be explained by the radiating plasmon (RP) model, where plasmons induced by resonant near-field interactions of fluorophores with metallic nanostructures (having dominant scattering properties) will radiate the spectral properties of the excited state intensely, thereby leading to observations of emission enhancements even from fluorophores with high free space quantum yields such as phycobiliproteins. Hence, on SiFs it is the apparent quantum efficiency of the combined excited-state fluorophore−metal complex that is of relevance, thus leading to the appearance of enhanced system quantum efficiencies when compared to the isolated fluorophore (system = excited-state fluorophore−metal complex). The RP model is described in greater detail in the Introduction.[26,27,36] Various other groups have also reported fluorescence emission enhancements between 20- and 50-fold for fluorescein dyes and CdSe/ZnS quantum dots on plasmonic nanostructures.[41,42] It is well known that fluorescein has a high quantum efficiency of approximately between 80 and 90% and CdSe/ZnS quantum dots have a quantum efficiency of approximately between 30 and 50%.[43−45] Hence, in these reports we see that the enhanced fluorescence signatures observed indicates an apparent system quantum efficiency greater than 100%, which supports our MEF results with phycobiliproteins.

The fluorescence intensity decay curves of the monolayer of R-phycoerythrin (R-PE) on a glass substrate and SiFs are shown in Figure 2. Also shown in the figure is the instrument response function (IRF). The solid lines indicate the best fit to the
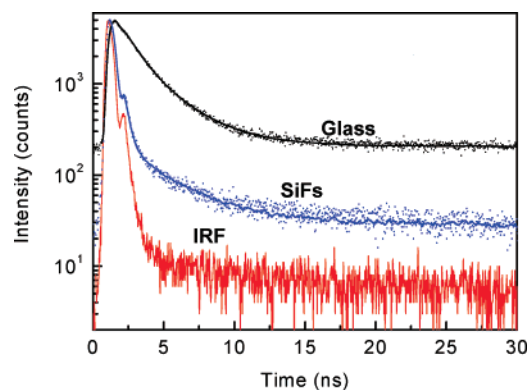

Figure 2. Fluorescence intensity decays from a monolayer of R-phycoerythrin on glass and SiFs. IRF = instrument response function. SiFs = silver island films.

TABLE 1: Lifetime Decay Parameters Obtained from a Monolayer of R-Phycoerythrin on Glass and SiFs

	α_1	τ_1 (nsec)	α_2	τ_2 (nsec)	χ^2	intensity-weighted lifetime τ (nsec)	amplitude-weighted lifetime τ (nsec)
glass	0.36	2.679	0.64	0.972	1.121	2.014	1.590
SiFs	0.02	3.07	0.98	0.144	1.088	1.143	0.214

experimental decay curves. As can be seen from the figure and the results tabulated in Table 1, the intensity decay of R-PE monolayers on SiFs is faster than observed on the glass control substrate. The amplitude weighted lifetime was found to decrease from 1.59 ns on the glass substrate to 0.21 ns on the SiFs substrate, a decrease of 7-fold. This shortening of lifetime on SiFs strongly supports that the increase in observed fluorescence intensity is due to the radiation from plasmons that are induced in the silver nanoparticles by the near-field excited fluorophores.[26,27,36] We also performed control experiments to verify that the short component in the intensity decay was not due to scattered light. The control measurements on the glass or SiFs substrates, without an R-PE monolayer, yielded a very weak signal in the time-correlated single-photon counting
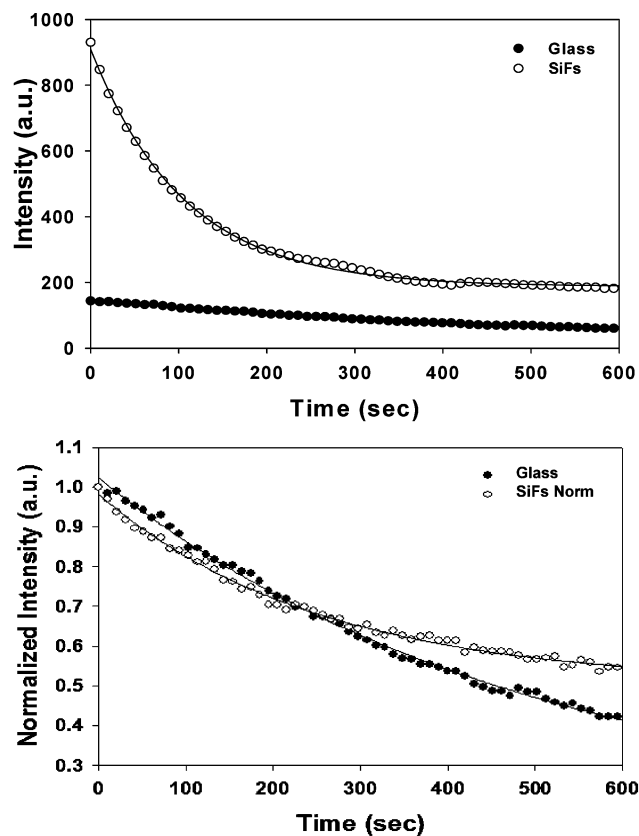
Figure 3. (Top) Steady-state fluorescence intensity decays from a monolayer of R-phycoerythrin on glass and SiFs. (Bottom) Normalized intensity decays for a monolayer of R-phycoerythrin on glass and SiFs after the incident laser power on SiFs was adjusted to match the *initial* fluorescence signal intensity on glass.

fluorescence lifetime spectrometer when observed through the combination of filters used to isolate the R-PE emission. We further examined the possibility of scattered light by recording the emission spectra through the emission filter sets used for the intensity-time decay measurements. These spectra showed again very weak intensity when excited at 473 nm, demonstrating that scattered light is not the origin of the short lifetime components of R-PE monolayers on SiFs.

Next, we measured the photostability of the monolayer of R-PE on both the glass substrate and the SiFs (Figure 3). Using the same incident laser power (10 mW), we observed significantly more fluorescence from the SiFs as compared to the glass control sample, when the integrated area under the respective curves is taken into consideration (Figure 3, top). This integration shows that the proteins on SiFs (when compared on glass) show an approximately 4-fold increase in total fluorescence emission over 10 min. However, when we attenuate the laser incident power on a SiFs to give the similar initial emission intensity as observed on the glass substrate, we see similar photostability characteristics. When this intensity decay is normalized to its respective value at $t = 0$ (Figure 3, bottom), it can be seen that the R-PE monolayers on SiFs are more photostable, as expected, than those in the case of the glass substrate.

We performed fluorescence emission and lifetime measurements on monolayers of the other four phycobiliproteins (B-PE, APC, XAPC, and C-PC). The results of these experiments are tabulated in Table 2. The table contains the enhancement factors on SiFs for the phycobiliproteins, the full width at half-maximum (fwhm) of the spectra on both glass and SiFs, and the intensity weighted and amplitude weighted lifetimes on glass

TABLE 2: Fluorescence Enhancement Factor, Full Width at Half-Maximum (fwhm) of Spectra, and Lifetime Parameters Obtained from a Monolayer of Phycobiliproteins on Glass and SiFs

	intensity enhancement factor	fwhm (nm)	intensity-weighted lifetime τ (nsec)	amplitude-weighted lifetime τ (nsec)
BPE SiFs	∼3	30	0.47	0.16
BPE glass	N/A	27	1.69	1.21
APC SiFs	N/A	45	0.27	0.22
APC glass	N/A	N/A	0.54	0.32
XAPC SiFs	∼9	31	0.37	0.27
XAPC glass	N/A	35	0.73	0.55
CPC SiFs	N/A	55	0.06	0.06
CPC glass	N/A	N/A	0.24	0.19

and SiFs of the proteins. The results indicate an approximately 3-fold increase in emission intensity, minimal change in fwhm of the emission spectra between SiFs and glass, and an approximately 7-fold decrease in lifetime of the monolayer of B-PE on SiFs when compared to the glass control. The results also show an approximately 9-fold increase in emission intensity, minimal change in fwhm of the emission spectra between SiFs and glass, and an approximately 2-fold decrease in the lifetime of the monolayer of XAPC on SiFs when compared to the glass control. We ensured that a uniform monolayer of these phycobiliproteins were formed on the surface of glass and SiFs by taking the measurements on several different areas on the sample and found comparable results. However, we encountered difficulties in the quality of the APC and C-PC monolayers formed on the glass substrates. Hence, we were unable to get neither satisfactory steady-state fluorescence emission spectra nor lifetime information from these samples. The discrepancy in behavior of these proteins is under investigation at this time. The enhancement factors observed for different batches of the monolayer of phycobiliproteins on SiFs was found to be between 5 and 10% of the reported values presented above and in Table 2. It is important to note that the deposition of phycobiliproteins onto SiFs as a monolayer has several implications: (i) because MEF is known to occur at distances of up to 90 nm from the silver surface,[32] the monolayer of phycobiliproteins provides us with the opportunity to test MEF from the proteins within this distance range; (ii) these results can inspire interest into further studies where phycobiliproteins can be used as labels in high-sensitivity surface bioassays, that is, MEF-based surface assays where various biorecognition events can be monitored on SiFs instead of glass substrates. For such assays, it is crucial to first establish that fluorescence emission from phycobiliproteins on SiFs is enhanced significantly when compared to glass.

However, we acknowledge that the monolayer results can raise the question of whether differences in phycobiliprotein attachment density between glass and SiF substrates affects the MEF that is observed. To eliminate this ambiguity, we have performed fluorescence emission and lifetime measurements with a thin liquid layer of the five phycobiliproteins sandwiched between two glass substrates separately (and a SiFs and glass substrate) clamped together. In this setup, we can expect the same volume of phycobiliproteins on the control and SiFs samples and thus negate the effect of any surface coverage issues. Figure 4 shows the fluorescence emission spectra from a thin liquid layer of R-phycoerythrin (R-PE) sandwiched between a glass substrate and SiFs and also the glass control substrate. The results show an approximately 6-fold increase in fluorescence intensity on SiFs, as compared to a control sample containing no surface silver nanostructures. The inset
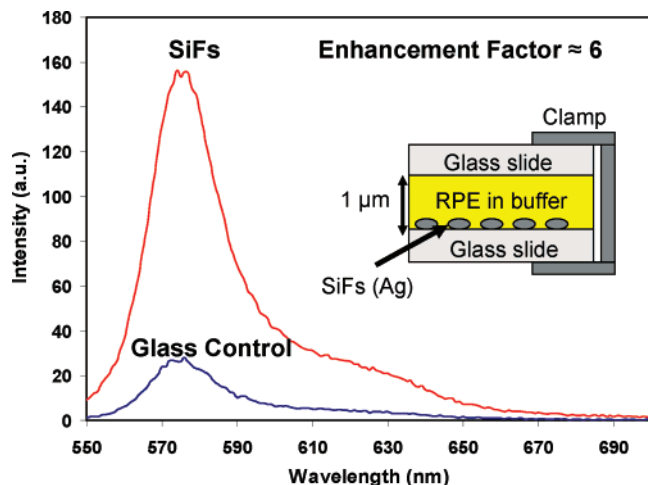
Metal-Enhanced Fluorescence of Phycobiliproteins

J. Phys. Chem. C, Vol. 111, No. 51, 2007 **18861**

Figure 4. Fluorescence spectra from a liquid sandwich of R-phycoerythrin on glass and SiFs. (Inset) Diagram showing experimental configuration.
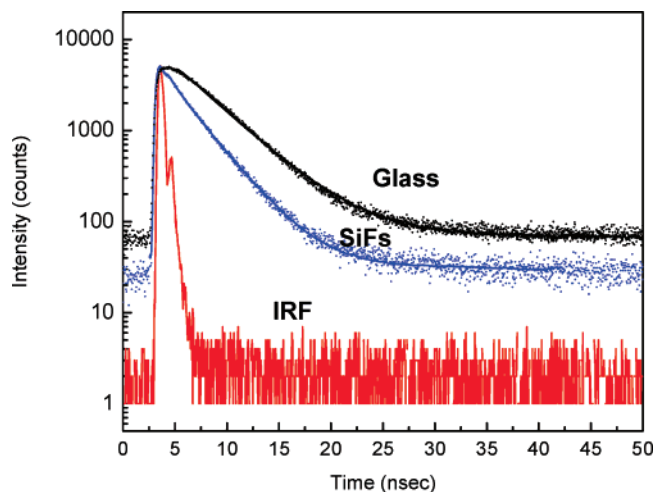

Figure 5. Fluorescence intensity decays from a liquid sandwich of R-phycoerythrin on glass and SiFs. IRF = instrument response function. SiFs = silver island films.

TABLE 3: Lifetime Decay Parameters Obtained from a Liquid Sandwich of R-Phycoerythrin on Glass and SiFs

	α_1	τ_1 (nsec)	α_2	τ_2 (nsec)	χ^2	intensity-weighted lifetime τ (nsec)	amplitude-weighted lifetime τ (nsec)
glass	1.00	4.158	N/A	N/A	1.574	4.158	4.158
SiFs	0.68	3.064	0.32	0.850	1.103	2.813	2.365

in the figure shows the experimental configuration. This finding suggests that this approach may be of significance for optically amplifying phycobiliprotein fluorescence-based bioassays, especially in flow cytometry applications where direct attachment of the phycobiliproteins to the silver nanostructures is not required.

The fluorescence intensity decay curves for the sandwiched liquid layer of R-phycoerythrin (R-PE) on glass and SiFs is shown in Figure 5. Also shown in the figure is the instrument response function (IRF). The solid lines indicate the best fit to the experimental decay curves. As can be seen from the figure and the results tabulated in Table 3, the intensity decay of R-PE monolayers on SiFs is faster than those on the glass substrate. The amplitude weighted lifetime was found to decrease from 4.16 ns on the glass substrate to 2.17 ns on the SiF substrate, a decrease of approximately 2-fold. We believe the shortening

TABLE 4: Fluorescence Enhancement Factor, Full Width at Half-Maximum (fwhm) of Spectra, and Lifetime Parameters Obtained from a Liquid Sandwich of Phycobiliproteins Studied on Glass and SiFs

	intensity enhancement factor	fwhm (nm)	intensity-weighted lifetime τ (nsec)	amplitude-weighted lifetime τ (nsec)
BPE SiFs	~6	22	2.77	2.55
BPE glass	N/A	22	4.13	4.13
APC SiFs	~5	26	1.70	1.68
APC glass	N/A	26	2.16	2.16
XAPC SiFs	~6	26	1.52	1.38
XAPC glass	N/A	26	2.08	2.08
CPC SiFs	~10	31	1.47	1.38
CPC glass	N/A	31	2.00	2.00

of lifetime on SiFs strongly suggests that the increase in observed fluorescence intensity is due to the radiation from plasmons that are induced on the silver nanoparticles by the excited fluorophores.[26,27,36] It is interesting that the decrease in lifetime of R-PE on SiFs when compared to glass is smaller for the liquid sample (as opposed to the monolayer). This could be due to the fact that in the liquid sample we are collecting the signal from approximately a 1-μm-thick liquid layer that is formed when the SiFs and the glass substrates are clamped. In this 1-μm-thick liquid layer, only the phycobiliproteins within the near field of the silver nanostructures (approximately <50 nm from the surface) experience the MEF effect.[21−25,] Hence, the majority of the excited protein molecules do not induce plasmons in the silver nanostructures to produce the MEF effect. As a result, the lifetimes are thought to originate from two distinct populations of the proteins, with the larger contribution from the molecules in free solution (bulk solution), and thus a smaller decrease in lifetime on SiFs is observed. Alternatively, *for the monolayer sample*, all of the phycobiliproteins are within the near field of the silver nanostructures and hence induce radiating plasmons in the silver nanoparticles, thus displaying a larger change in lifetime on SiFs. (Table 3 for liquid sandwich samples show $\alpha_1 = 0.68$, $\alpha_2 = 0.32$ for SiFs, and Table 1 for monolayer samples show $\alpha_1 = 0.02$, $\alpha_2 = 0.98$ for SiFs.)

We performed similar experiments on sandwiched liquid layers for the four other phycobiliproteins (B-PE, APC, XAPC, and C-PC). The results of these experiments are tabulated in Table 4. They indicate an approximately 6-fold increase in emission intensity, no change in fwhm of the emission spectra between SiFs and glass, and an approximately 2-fold decrease in lifetime of the sandwich liquid layer of B-PE on SiFs, as compared to glass. The results show an approximately 5-fold increase in emission intensity, no change in fwhm of the emission spectra between SIF and glass, and an approximately 1.4-fold decrease in lifetime of the sandwich liquid layer of APC on SiFs, as compared to glass. The results also show an approximately 6-fold increase in emission intensity, no change in fwhm of the emission spectra between SiFs and glass, and an approximately 1.5-fold decrease in lifetime of the sandwich liquid layer of XAPC on SiFs, as compared to glass. Finally, we see an approximately 10-fold increase in emission intensity, no change in fwhm of the emission spectra between SiFs and glass, and an approximately 1.4-fold decrease in lifetime of the sandwich liquid layer of C-PC on SiFs, as compared to glass. The enhancement factors observed for different batches of the sandwiched liquid layers of phycobiliproteins on SiFs was found to be approximately within 5% of the reported values presented above and in Table 4.

The enhanced luminescence can also be seen visually on the glass and SiFs (Figure 6, top), from photographs of the
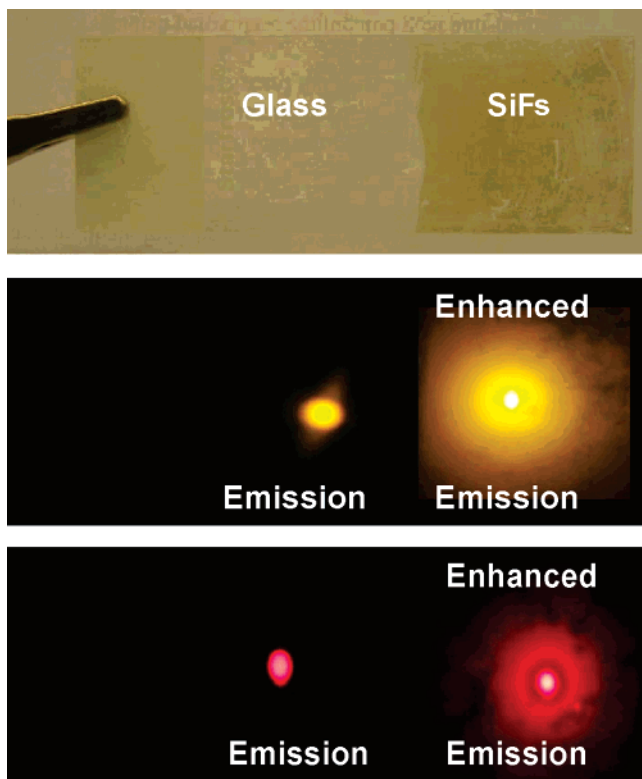
18862 *J. Phys. Chem. C, Vol. 111, No. 51, 2007*

Chowdhury et al.

Figure 6. Photographs of silver island films (SiFs) deposited on a glass substrate (top). Emission of R-phycoerythrin on glass and SiFs (middle). Emission of cross-linked allophycocyanin on glass and SiFs (bottom).

fluorescence emission of a monolayer of R-PE (Figure 6, middle) and XAPC (Figure 6, bottom) on these substrates. The fluorescence images were taken with the appropriate longpass filters in front of the camera in order to block the excitation light. These photographs clearly show the MEF effect of the silver nanostructures on the phycobiliprotein monolayer, providing compelling visual evidence of the enhanced emission from the silver.

4. Conclusions

In this study, we have shown that plasmonic metal nanostructures such as silver island films (SiFs) can be used to enhance the fluorescence emission from phycobiliproteins. The experiments were performed in two different formats, namely with a monolayer of the proteins self-assembled on glass and SiFs, and on a thin liquid layer of the proteins sandwiched in between two glass substrates, and a SiFs and a glass substrate that were clamped. Our results show a maximum of ~9-fold increase in fluorescence intensity from a monolayer of the proteins on SiFs combined with a maximum ~7-fold decrease in lifetime. In the monolayer configuration, we also show increased photostability of the phycobiliproteins on SiFs, as compared to the glass control samples. Hence, our results indicate that metal-enhanced fluorescence (MEF) can be utilized to increase the sensitivity of various fluoro-immunoassays that employ phycobiliproteins as their fluorescence labels. The sensitivity enhancement can potentially be achieved by tethering the assay constituents (such as capture antibodies) on SiFs instead of the currently used substrates. We also show a maximum of 10-fold increase in fluorescence intensity from a sandwiched liquid layer of the proteins on SiFs and a maximum of 2-fold decrease in the lifetime. These results indicate that enhancement of phycobiliprotein emission can even be attained

without chemical linkage of the proteins to the SiFs. The results of this study strongly suggests that metal-enhanced fluorescence (MEF) can be employed to increase the sensitivity of biological applications that employ phycobiliproteins as fluorescence labels such as flow cytometry, where biomolecules can flow through microchannels that are potentially coated with SiFs or other silver nanostructures, with no chemical linkage between the silver and the molecules. To the best of our knowledge, this is the first report of metal-enhanced fluorescence (MEF) from phycobiliproteins, and work is currently underway in our laboratories in applying the MEF effect on bioassays employing phycobiliprotein probes.

References and Notes

(1) Sun, L.; Wang, S.; Chen, L.; Gong, X. *IEEE J. Sel. Top. Quantum Electron.* **2003**, *9*, 177−188.

(2) Oi, V. T.; Glazer, A. N.; Stryer, L. *J. Cell Biol.* **1982**, *93*, 981−986.

(3) Glazer, A. N.; Stryer, L. *Biophys. J.* **1983**, *43*, 383−386.

(4) Isailovic, D.; Sultana, I.; Phillips, G. J.; Yeung, E. S. *Anal. Biochem.* **2006**, *358*, 38−50.

(5) Gaigalas, A.; Gallagher, T.; Cole, K. D.; Singh, T.; Wang, L.; Zhang, Y-Z. *Photochem. Photobiol.* **2006**, *82*, 635−644.

(6) Wolf, E.; Schübler, A. *Plant Cell Environ.* **2005**, *28*, 480−491.

(7) Chen, Z.; Kaplan, D. L.; Yang, K.; Kumar, J.; Marx, K. A.; Tripathy, S. K. *Appl. Opt.* **1997**, *36*, 1655−1659.

(8) Guard-Friar, D.; MacColl, R.; Berns, D. S.; Wittmershaus, B.; Knox, R. S. *Biophys. J.* **1985**, *47*, 787−793.

(9) Brody, S. S. *Photosynth. Res.* **2002**, *73*, 127−132.

(10) Trinquet, E.; Maurin, F.; Préaudat, M.; Mathis, G. *Anal. Biochem.* **2001**, *296*, 232−244.

(11) Kronick, M. N.; Grossman, P. D. *Clin. Chem.* **1983**, *29/9*, 1582−1586.

(12) Loos, D.; Cotlet, M.; Schryver, F. D.; Habuchi, S.; Hofkens, J. *Biophys. J.* **2004**, *87*, 2598−2608.

(13) Lakowicz, J. R. *Principles of Fluorescence Spectroscopy*; Springer: New York, 2006.

(14) Wellman, A.; Sepaniak, M. J. *Anal. Chem.* **2006**, *78*, 4450−4456.

(15) Batard, P.; Szollosi, J.; Luescher, I.; Cerottini, J-C.; MacDonald, R.; Romero, P. *Cytometry* **2002**, *48*, 97−105.

(16) Triantafilou, K.; Triantafilou, M.; Wilson, K. *Cytometry* **2000**, *41*, 226−234.

(17) Wilson, K. M.; Morrison, I. E. G.; Smith, P. R.; Fernandez, N.; Cherry, R. J. *J. Cell Sci.* **1996**, *109*, 2102−2109.

(18) Wu, M.; Goodwin, P. M.; Ambrose, W. P.; Keller, R. A. *J. Phys. Chem.* **1996**, *100*, 17406−17409.

(19) Ma, Y.; Shortreed, M. R.; Yeung, E. S. *Anal. Chem.* **2000**, *72*, 4640−4645.

(20) Drexhage, K. H. *Progress in Optics*; North-Holland: Amsterdam, 1974; pp 161−232.

(21) Lakowicz, J. R. *Anal. Biochem.* **2001**, *298*, 1−24.

(22) Lakowicz, J. R.; Shen, Y.; D'Auria, S.; Malicka, J.; Fang, J.; Gryczynski, Z.; Gryczynski, I. *Anal. Biochem.* **2002**, *301*, 261−277.

(23) Matveeva, E.; Gryczynski, Z.; Malicka, J.; Gryczynski, I.; Lakowicz, J. R. *Anal. Biochem.* **2004**, *334*, 303−311.

(24) Zhang, J.; Matveeva, E.; Gryczynski, I.; Leoneko, Z.; Lakowicz, J. R. *J. Phys. Chem. B* **2005**, *109*, 7969−7975.

(25) Zhang, J.; Malicka, J.; Gryczynski, I.; Lakowicz, J. R. *J. Phys. Chem. B* **2005**, *109*, 7643−7648.

(26) Geddes, C. D.; Lakowicz, J. R. *J. Fluorsc.* **2002**, *12*, 121−129.

(27) Aslan, K.; Leonenko, Z.; Lakowicz, J. R.; Geddes, C. D. *J. Phys. Chem. B* **2005**, *109*, 3157−3162.

(28) Aslan, K.; Lakowicz, J. R.; Geddes, C. D. *J. Phys. Chem. B* **2005**, *109*, 6247−6251.

(29) Aslan, K.; Gryczynski, I.; Malicka, J.; Matveeva, E.; Lakowicz, J. R.; Geddes, C. D. *Curr. Opin. Biotechnol.* **2005**, *16*, 55−62.

(30) Zhang, J.; Lakowicz, J. R. *J. Phys. Chem. B* **2006**, *110*, 2387−2392.

(31) Ray, K.; Badugu, R.; Lakowicz, J. R. *J. Phys. Chem. B* **2006**, *110*, 13499−13507.

(32) Ray, K.; Badugu, R.; Lakowicz, J. R. *Langmuir* **2006**, *22*, 8374−8378.

(33) Fu, Y.; Lakowicz, J. R. *Anal. Chem.* **2006**, *78*, 6238−6245.

(34) Fu, Y.; Lakowicz, J. R. *J. Phys. Chem. B* **2006**, *110*, 22557−22562.

(35) Aslan, K.; Huang, J.; Wilson, G. M.; Geddes, C. D. *J. Am. Chem. Soc.* **2006**, *128*, 4206−4207.

(36) Lakowicz, J. R. *Anal. Biochem.* **2005**, *337*, 171−194.

(37) Aslan, K.; Leonenko, Z.; Lakowicz, J. R.; Geddes, C. D. *J. Fluoresc.* **2005**, *15*, 643−654.

(38) Mie, G. *Ann. Phys.* **1908**, *25*, 377−445.

(39) Kreibig, U.; Vollmer, M. *Optical Properties of Metal Clusters*; Springer-Verlag: New York, 1995.

(40) Malicka, J.; Gryczynski, I.; Geddes, C. D.; Lakowicz, J. R. *J. Biomed. Opt.* **2003**, *8*, 472−478.

(41) Solokov, K.; Chumanov, G.; Cotton, T. M. *Anal. Chem*. **1998**, *70*, 3898−3905.

(42) Song, J.-H.; Atay, T.; Shi, S.; Urabe, H.; Nurmikko, A. V. *Nano Lett.* **2005**, *5*, 1557−1561.

(43) Hulspas, R.; Krijtenburg, P. J.; Keij, J. F.; Bauman, J. G. J. *J. Histochem. Cytochem.* **1993**, *41*, 1267−1272.

(44) Hines, M. A.; Guyot-Sionnest, P. *J. Phys. Chem*. **1996**, *100*, 468−471.

(45) Rodriguez-Viejo, J.; Jensen, K. F.; Mattoussi, H.; Michel, J.; Dabbousi, B. O.; Bawendi, M. G. *Appl. Phys. Lett*. **1997**, *70*, 2132−2134.